



ELSEVIER

Contents lists available at ScienceDirect

Physica B

journal homepage: [www.elsevier.com/locate/physb](http://www.elsevier.com/locate/physb)

# Electron transport mechanism of thermally oxidized ZnO gas sensors

N.H. Al-Hardan\*, M.J. Abdullah, A. Abdul Aziz

School of Physics, Universiti Sains Malaysia (USM), 11800 Minden, Pulau Pinang, Malaysia

## ARTICLE INFO

### Article history:

Received 11 June 2010

Received in revised form

27 July 2010

Accepted 6 August 2010

### Keywords:

Electrical conductivity

Gas sensors

Oxidation process

ZnO

## ABSTRACT

ZnO gas sensor was fabricated by thermal oxidation of metallic Zn at different time periods. The sensors were characterized by *I*–*V* measurement with DC voltage, ranging from –2 to 2 volts, in both normal air and H<sub>2</sub> gas with concentration from 40 to 160 ppm. The transport mechanism of the carriers was found to be due to thermionic process through both the grain boundaries and the metal–semiconductor junctions. Resistance of the ZnO sensing film is independent of applied voltage in the range  $0.5\text{ V} < V_a < 2\text{ V}$ ; however, it is dependent on gas concentration, which makes it useful for gas sensing application.

© 2010 Elsevier B.V. All rights reserved.

## 1. Introduction

Metal oxide devices change their resistivity in the presence of reducible or oxidation gases. They have been used since 1971, when Taguchi [1] introduced to the market its metal oxide gas sensor based on tin dioxide (SnO<sub>2</sub>) thick films. Many published works tried to explain the mechanism involved in the gas detection process. Most of these works depend on measuring the change of resistance as a function of the gas concentration (sensitivity) and type of gas (selectivity). The method essentially detects the sum of different effects that occur on the surface of the sensor that is attributed to the grain, grain boundary, and metal–semiconductor contacts [2].

Various metal oxides have been investigated for gas sensing applications. These include titanium oxides (TiO<sub>2</sub>) [3], vanadium pentoxides (V<sub>2</sub>O<sub>5</sub>) [4], SnO<sub>2</sub> [5], tungsten oxides (WO<sub>3</sub>) [6], and zinc oxide (ZnO) [7]. It appears that SnO<sub>2</sub> and ZnO have received more attention because of their nontoxic, relatively good, and stable electrical properties.

ZnO thin film has been extensively studied because of its diverse applications in different modern technological fields, such as gas sensors [7], conductive transparent layers for solar cell and displays application, and surface acoustic wave sensors. They can be prepared by different methods, such as DC and RF sputtering, sol–gel and thermal pyrolysis [8], and oxidation of Zn precursor, such as ZnS and Zn [9,10].

This study investigates the electron transport mechanism of the ZnO gas sensor in the presence of different concentrations of

H<sub>2</sub> based on the thermo-emission theory. The study focuses the current–voltage and resistance–voltage characteristics of the gas sensor at voltage range –2 to 2 V.

## 2. Experimental method

An n-type Si (1 0 0) wafer was used as a substrate. The wafers were initially cleaned with RCA standard method and thermally oxidized at 1100 °C for 4 h in oxygen flow to form 1.2 μm of silicon dioxide (SiO<sub>2</sub>). Photolithography was employed to pattern the Ti/Pt heat element and the conducting electrodes. Ti and Pt were coated using the Edwards A306 DC magnetron sputtering unit, followed by wet etching process to obtain the final device. (Fig. 1 shows the device diagram.) Thin films of Zn metal were coated with a good uniformity over the Ti/Pt electrodes using high-purity (99.99%) Zn target by the same unit. The ultimate pressure of the unit was  $1 \times 10^{-5}$  Torr and was raised to  $4 \times 10^{-3}$  Torr during the deposition process by flowing high-purity Ar (99.999%).

Thermal oxidation of the Zn films was carried out in a horizontal controlled tube furnace; the samples were introduced into the furnace at room temperature. The temperature was then raised at the rate of  $5\text{ °C min}^{-1}$  to 400 °C in high-purity O<sub>2</sub> (99.99%) atmosphere for 30 and 60 min. The thickness of the ZnO thin film was 0.3 μm as measured by the optical method using Filmetrics model F20 (Filmetrics Inc., San Diego, CA, USA).

The *I*–*V* characteristic of the produced device was measured using a programmable electrometer—model 617 KEITHLEY. The applied voltage  $V_a$  (–2 to 2) V from the electrometer was supplied to the measuring electrodes and the current was measured through the same unit. DC power supply (Lodestar 30V/3A) was used to supply voltage to the heating elements.

\* Corresponding author. Tel.: +60 17 4961778; fax: +60 4 6579150.  
E-mail address: [naif.zd06@student.usm.my](mailto:naif.zd06@student.usm.my) (N.H. Al-Hardan).

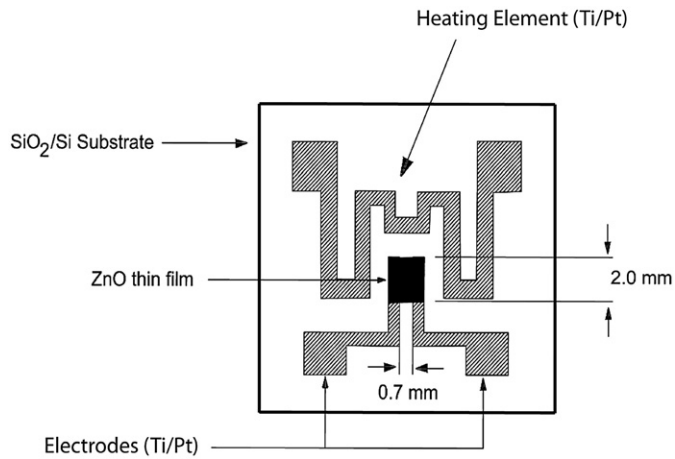


Fig. 1. Schematic layout structure of ZnO gas sensor; the sensing element's dimension is 2 mm × 2 mm.

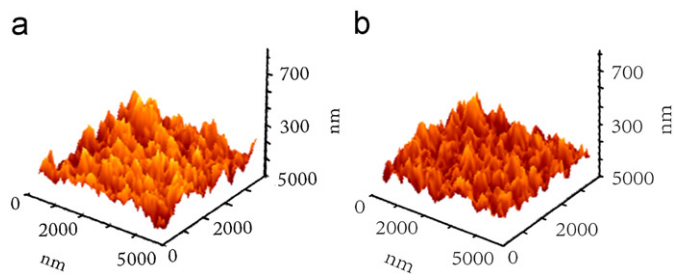


Fig. 2. AFM image of oxidized Zn for (a) 30 min and (b) 60 min.

Temperature of the heating element was controlled by varying the voltage and measured by a calibrated K-type thermocouple, which was mounted on the device to sense temperature of the sensor. The temperature of the sensor was maintained at 400 °C [11]. All the measurements were taken at room temperature (23 °C) and 62% humidity.

The test chamber was made of stainless steel, with a total volume of about 8200 cm<sup>3</sup>. A high grade gas mixture of 2% hydrogen and nitrogen (as buffer gas) was used for testing the device. H<sub>2</sub> gas concentrations inside the gas testing chamber were controlled by changing flow rate of the gas mixture, which was fed to the testing chamber [11–13]. Flow rate of the gas was controlled and measured through a mass flow controller (Cole-Parmer model 32708-26). To ensure a homogenous distribution of the gas under test in the chamber, the measurements were commenced 3 min after turning on the gas flow. After testing each gas concentration, the chamber was flushed using a commercial air pump, such that the air flow was passed through a glass vessel containing silica grains to ensure that the air supplied was dried.

X-ray diffraction (XRD) and atomic force microscopy (AFM) were used to determine the structure and morphology of the film sensor, respectively.

### 3. Results and discussion

#### 3.1. Structure and morphology

The surface morphology of the ZnO film as observed from the AFM (Fig. 2) micrographs proved that the grains are uniformly distributed within the scanning area, with individual columnar grains extending upwards. This surface characteristic is important for applications such as gas sensors and catalysts [14]. The root

mean square (rms) of surface roughness of the prepared films showed no significant difference in the surface roughness between two samples (30 and 60 min oxidation), which was about 45 ± 2 nm. XRD of the oxidized films is shown in Fig. 3, from which it can be observed that the films were polycrystalline. There is no evidence of Zn metal in the oxidized films, which confirmed the complete conversion of Zn metal to ZnO during oxidation.

The observed peaks were at the Bragg angles of 31.9°, 34.5°, 36.36°, 47.72°, and 56.74°, which represent the (1 0 0), (0 0 2), (1 0 1), (1 0 2), and (1 1 0) phases of ZnO (JCPDF card no. 36-1451), respectively. There was no observable difference in the XRD spectrum of the two ZnO films prepared at different oxidation times, which confirmed the results obtained by Alivov et al. [15], who prepared ZnO through the same method.

#### 3.2. Electrical properties

The current–voltage characteristic of the ZnO thin film is shown in Fig. 4. It is obvious that current is enhanced with the H<sub>2</sub> concentration, but better resolution of the measured current was obtained for the 30 min sample (Fig. 4(a)). For samples prepared for 60 min oxidation (Fig. 4(b)), the current change shows some evidence of saturation behavior at high H<sub>2</sub> concentrations, which suggests that the donor concentration begins to be limited, the same behavior that was also observed by Kim et al. [16]. It was suggested earlier that samples with longer oxidation time show less oxygen vacancies [11,17].

It was also found that the measured current of the sample prepared at 60 min was higher than that prepared at 30 min. It was suggested earlier [11,18] that sensitivity of the ZnO gas sensor can be enhanced by reducing carrier concentration (higher resistance); the increase of oxidation time from 30 to 60 min results in a decrease of oxygen vacancies and zinc interstitials in the samples, which led to a decrease of carrier concentrations, wider depletion layer, and higher potential energy between the grains.

The increase in applied voltage ( $V_a$ ) results in the lowering of barrier height at the grain boundaries thus it enhances the output current. In addition, the increase in H<sub>2</sub> concentration causes a reduction in barrier height between the grain boundaries and enhances the current [19] as more electrons are released.

The oxygen-vacancy model may be used to explain the reaction mechanisms in this case [11,20], in which the oxygen vacancies act as electron donors. The increase of oxidation time

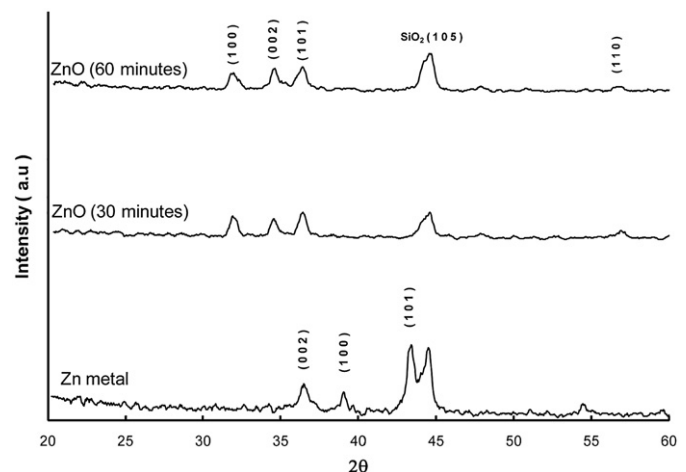


Fig. 3. XRD of the prepared ZnO films oxidized at 400 °C for 30 and 60 min in oxygen flow.

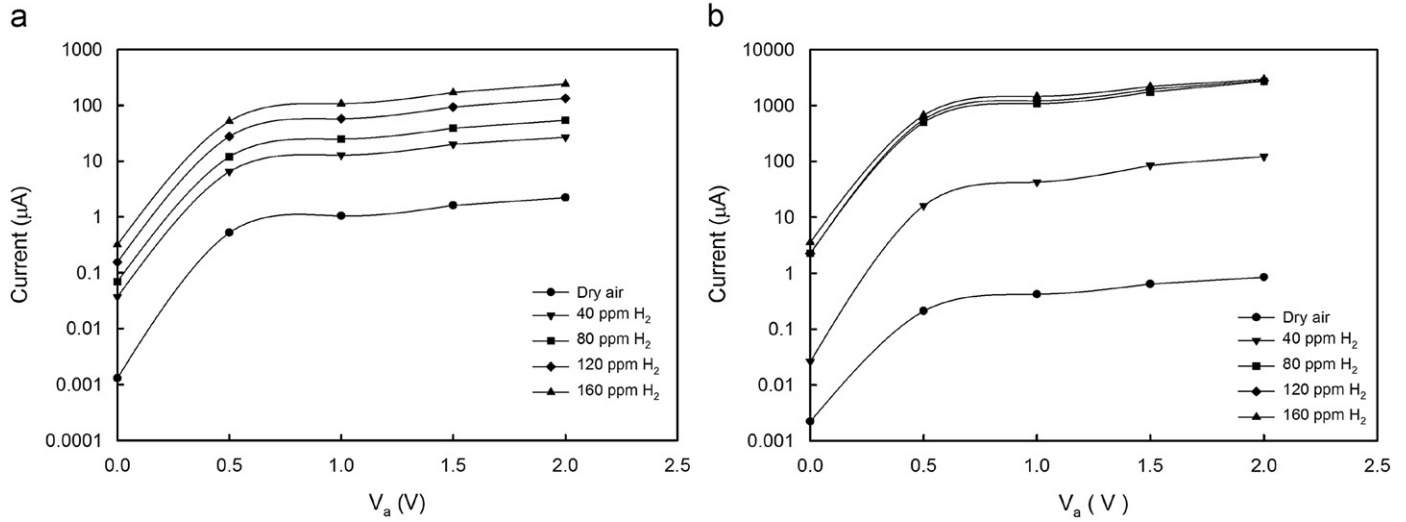
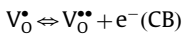
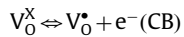
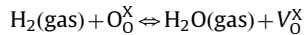


Fig. 4. Forward current–voltage characteristic of ZnO gas sensor oxidized at (a) 30 min and (b) 60 min for different H<sub>2</sub> concentrations, at the operating temperature of 400 °C.

from 30 to 60 min resulted in a decrease of the oxygen vacancies in the sample [17]. The reaction of hydrogen molecules with the oxygen can be expressed as follows: the hydrogen first reacted with the oxygen from the ZnO surface and as a consequence water vapor molecules and oxygen vacancies are produced. Consequently the oxygen vacancies became ionized due to the charge imbalance of the oxygen site, thereby electrons are introduced into the conduction band that consequently increased the measured current of the sensor. Thus for the sample with higher oxygen concentrations (lower oxygen vacancies) following 60 min oxidation, more reaction with hydrogen gas took place, thereby resulting in enhancement of the current response of the sensor. These reactions could have occurred as in the following steps according to Kröger–Vink notation [20]:



where  $O_0^X$  is the neutral oxygen from the surface,  $V_0$  the oxygen vacancy,  $V_0^X$  neutral oxygen vacancy,  $V_0^\bullet$  singly ionized oxygen vacancy,  $V_0^{\bullet\bullet}$  doubly ionized oxygen vacancy, and  $e^-(\text{CB})$  is the electrons at the conduction band.

The electron transport mechanism can be modeled based on the work of Pitcher et al. [6], which showed that the mechanism depends on carrier concentration of the semiconductor.

At low carrier concentration, width of the potential barrier is large and only electrons of sufficient kinetic energy are able to move over the barrier. At high carrier concentration, electrons will have the ability to tunnel through the narrow potential barrier. The first mechanism is known as thermionic emission, which is dominant for the Schottky contacts, while the second one is ascribed to electron tunneling [21].

Due to the increase of carrier concentration as a result of applied voltage and (or) H<sub>2</sub> concentration, the tunneling current becomes more significant and superimposes on pure thermionic emission current, which lowers the Schottky barrier height.

The theoretical resistance–voltage (*R–V*) characteristic associated with thermionic emission and electron tunneling mechanism is shown in Fig. 5 [6].

Fig. 6 shows the *R–V* characteristic obtained for the ZnO gas sensor, from which it can be inferred that electron transport in the gas sensor resembles the thermionic process. At low applied voltage  $-0.5 \text{ V} < V_a < 0.5 \text{ V}$ , the resistance of the film is not

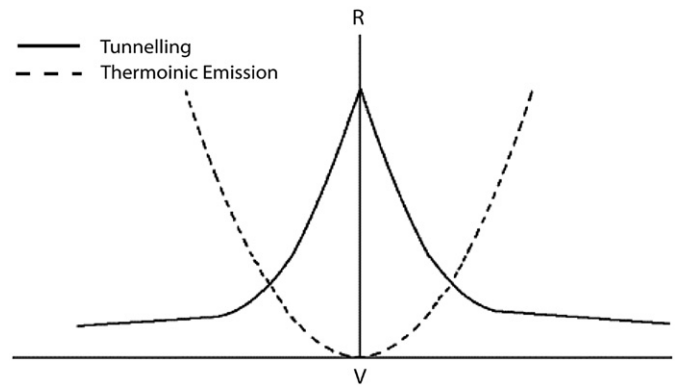


Fig. 5. Theoretical *R–V* characteristics associated with thermionic emission and tunneling [6].

constant for both samples, which means that the *I–V* curves are not linear. For voltage  $0.5 \text{ V} < V_a < 2 \text{ V}$ ,  $-2 \text{ V} < V_a < -0.5 \text{ V}$ , the resistance of each sample is almost constant (independent on voltage). In this region, H<sub>2</sub> concentration affects resistance of the sensing element; the higher the concentration, the lower the resistance. This dependence is very useful in gas sensing application and widely used for the determination of gas concentration in the atmosphere.

The linear dependence of resistance on gas concentration for the samples with 30 min of thermal oxidation is better than that of the 60 min samples, which can be applied for sensing H<sub>2</sub> concentration in the present studied range. For samples with 60 min of oxidation, good resistance resolution appears only in the concentration range less than 80 ppm. The near saturation in resistance magnitudes (above 80 ppm) for this sample suggests that the donor concentration begins to be limited [16].

#### 4. Conclusion

The electron transport of ZnO gas sensor prepared by thermal oxidation of Zn metal is attributed to the thermionic emission mechanism. Resistance of the sensor decreased with H<sub>2</sub> concentration in the range 40–160 ppm. The sensors prepared for 30 min oxidation show better sensing characteristics as compared with that of the sensors prepared for 60 min oxidation.

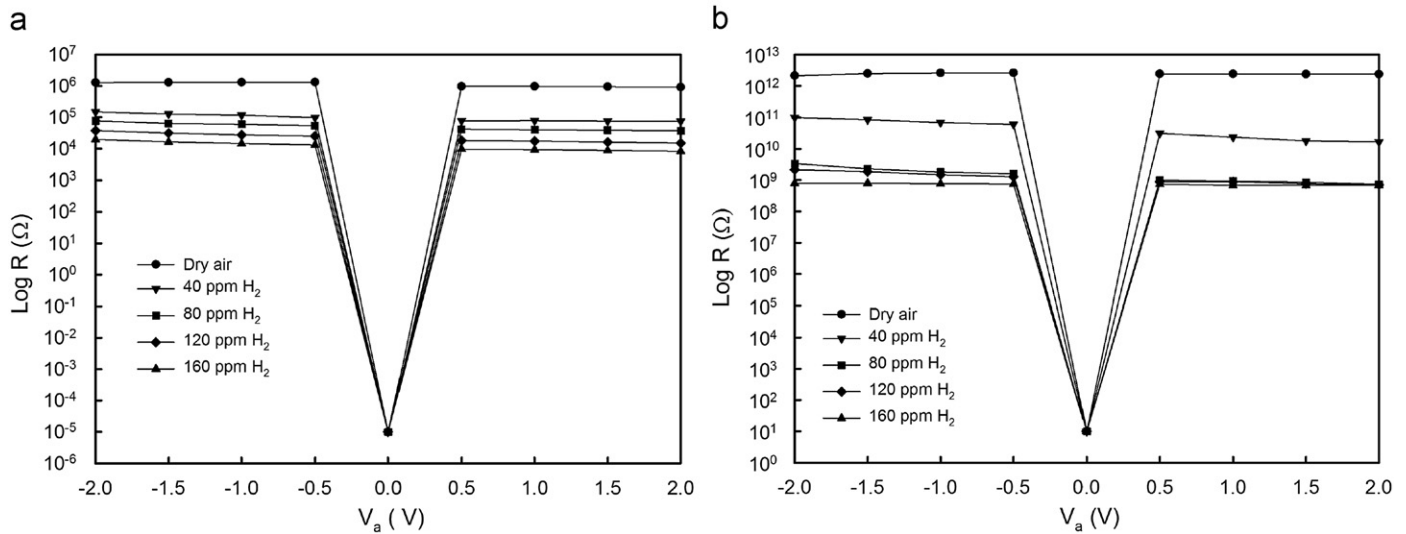


Fig. 6. R–V characteristic of the ZnO gas sensor for (a) 30 min and (b) 60 min samples.

### Acknowledgment

This work has been supported by Universiti Sains Malaysia (Penang, Malaysia) through a short term grant. N.H. Al-Hardan is grateful for the fellowship from the Institute of Graduate Studies, Universiti Sains Malaysia.

### References

- [1] N. Taguchi, US Patent 3,625,756, December 1971.
- [2] P.T. Mosely, B.C. Tofield, in: *Solid State Gas Sensor*, Adam Hilger, Bristol and Philadelphia, 1987.
- [3] Y. Hayakawa, K. Iwamoto, Kikuta, S. Hirano, *Sensors Actuators B* 62 (2000) 55.
- [4] O. Schilling, K. Colbow., *Sensors Actuators B* 21 (1994) 151.
- [5] K.H. Cha, H.C. Park, K.H. Kim, *Sensors Actuators B* 21 (1994) 91.
- [6] S. Pitcher, J.A. Thiele, H. Ren, J.F. Vetelino, *Sensors Actuators B* 93 (2003) 454.
- [7] P.P. Sahay, *J. Mater. Sci.* 40 (2005) 4383.
- [8] Ü. Özgür, Y.I. Alivov, C. Liu, A. Teke, M.A. Reshchikov, S. Doğan, V. Avrutin, S.J. Cho, H. Morkoç, *J. Appl. Phys.* 98 (2005) 041301.
- [9] S. Cho, J. Ma, Y. Kim, Y. Sun, G.K.L. Wong, J.B. Ketterson, *Appl. Phys. Lett.* 75 (1999) 2761.
- [10] X.T. Zhang, Y.C. Liu, Z.Z. Zhi, J.Y. Zhang, Y.M. Lu, W. Xu, D.Z. Shen, G.Z. Zhong, X.W. Fan, X.G. Kong, *J. Cryst. Growth* 240 (2002) 463.
- [11] N. Al-Hardan, M.J. Abdullah, A. Abdul Aziz, *Appl. Surf. Sci.* 255 (2009) 7794.
- [12] Gas Testing Box Model no. SR3, Instruction Manual, Figaro Sensor Company, <www.figarosensor.com>.
- [13] N. Al-Hardan, M.J. Abdullah and A. Abdul Aziz, *Adv. Appl. Ceram.*, Doi:10.1179/174367510X12722693956275, in press.
- [14] Z Dachun, Q Zhongkai, P Xiaoren, D Muji, S. Minggen, *J. Vac. Sci. Technol. B* 15 (1997) 805.
- [15] Y.I. Alivov, A.V. Chernykh, M.V. Chukichev, R.Y. Koroptkov, *Thin Solid Films* 473 (2005) 241–246.
- [16] S. Kim, B.S. Kang, F. Ren, K. Ip, Y.W. Heo, D.P. Norton, S.J. Pearton, *Appl. Phys. Lett.* 84 (2004) 1698.
- [17] V. Khranovskyy, J. Eriksson, A. Lloyd-Spetz, R. Yakimova, L. Hultman, *Thin Solid Films* 517 (2009) 2073.
- [18] J.B.K. Law, J.T.L. Thong, *Nanotechnology* 19 (2008) 205502.
- [19] N. Barsan, U. Weimar, *J. Electroceram.* 7 (2001) 143.
- [20] A. Gurlo, R. Riedel, *Angew. Chem. Int. Ed.* 46 (2007) 3826.
- [21] E.H. Rhoderick, R.H. Williams, in: *Metal–semiconductor contacts*, Clarendon, Oxford, 1988.